Publications of the Institute of Geophysics, Polish Academy of Sciences
Geophysical Data Bases, Processing and Instrumentation
vol. 442 (D-77), 2022, pp. 5–17
DOI: 10.25171/InstGeoph_PAS_Publs-2022-022

Dynamic and Electric Charge Structure of Thunderclouds Obtained from the WRF and WRF_ELEC Models and Related to the Charge Sources of Multiple CG Flashes Detected by the LLDN in the Warsaw Region during Thunderstorm Season in 2009

Piotr BARAŃSKI✉ and Jakub GUZIKOWSKI

Institute of Geophysics, Polish Academy of Sciences, Warsaw, Poland
✉ baranski@igf.edu.pl

Abstract

The paper presents the results of spatial location (in the coordinates of the local and rectangular Cartesian system: *x*, *y*, *z*) as well as the polarity and electric charge of all sources in thunderclouds discharged by individual return strokes during 17 multiple cloud-to-ground discharges recorded simultaneously by six measurement stations of the LLDN (Local Lightning Detection Network) system located in the Warsaw region in the spring and summer season of 2009. The post-time analysis of the collected digital electric field records of these discharges was carried out based on our own calculation algorithms, described in detail by Baranski et al. (2012). In turn, for two selected discharges from this group, one positive double ground flash from the 25 June 2009 storm and the other negative threefold ground flash from the 5 July 2009 storm, the supplementary simulations of radar reflectivity, the structure of the wind field and the thundercloud electric charge density were obtained from the WRF and WRF_ELEC models. Due to this, it was possible to distinguish with the time resolution up to 1 minute such regions of the thundercloud in which the simulated wind field and electric charge densities with different polarity created favourable conditions to initiate all return strokes of the considered multiple ground flashes and detected by the LLDN network. It also should be noted that the time resolution in the available routine radar observations from the IMWM-NRI is by one order of magnitude worse than the one delivered by the WRF simulations and amounts to 10 minutes.

Keywords: multiple ground flash, return stroke, lightning detection, thundercloud, WRF and WRF_ELEC models.

1. INTRODUCTION

In summer 2009 we have successfully operated the Local Lightning Detection Network (LLDN) in the Warsaw region that was consisting of 6 E-field measurements performed at the ground surface. The aim of this net was to provide an additional and complementary source of CG lightning data that allowed to evaluate 3D locations of point electric charge sources, i.e., to estimate parameters *x*, *y*, *z* in the local set of Cartesian coordinates, and the magnitude of the electric charge, *Q*, involved the lightning return strokes (RS) and continuing current (CC) of the considered multiple CGs (Baranski et al. 2012). Now, taking the possibility to use the WRF_ELEC model for the refining the dynamic and electric charge structure of thunderstorms occurring in Warsaw region in that time, we have made the comparison of how these two different methods are related to each other in the description/presentation of electric build up of the same thundercloud and in time when we were able to record lightning flash incident by the LLDN and initiated by this cloud.

The WRF_ELEC is an additional module dedicated to the Weather Research and Forecasting numerical model (WRF). It contains the basic electrification microphysics parameterization scheme prepared by the National Severe Storms Lab (NSSL) from Norman, Oklahoma, USA. The WRF is a system defined for numerical simulation of atmospheric processes and weather forecast. Its dynamic solver is based on the three-dimensional compressible non-hydrostatic equations and the charge separation schemes therein are used according to description presented first by Mansell et al. (2005).

In recent years many papers were published to show how using the extended and constantly modified numerical models connected to the WRF group, for example WRF_ELEC or WRF-ARW models, can improve and broaden the study of the dynamic and electric charge structure evolution of different and complex thunderstorm systems in the USA (Mansell et al. 2010; Fierro et al. 2013). Such models have simulated the particular and characteristic stages of thundercloud electric and dynamic development with a high resolution in space and time domain by the application of the explicit electrification and lightning parameterizations to the post-time analysis of the considered thunderstorm cases. It is worth noting that the simulated bulk lightning activity for different types of thunderstorm systems occurring in the USA and obtained from the WRF models have exhibited overall good qualitative agreement with the lightning detection and location data delivered by the Earth Networks Total Lightning Network (ENTLN) for the considered severe thunderstorm episodes.

2. LLDN PERFORMANCE AND CONFIGURATION

In summer 2009 the Local Lightning Detection Network (LLDN) in the Warsaw region was set up as the result of the research project No. COST/204/2006 granted by the Polish Ministry of Science and Higher Education. In that time this net consisted of six E-field measurement stations that were located at different and distant places in the Warsaw region. Such net configuration is shown in Fig. 1 and the exemplary general view of one LLDN station is given in Fig. 2. Each LLDN measuring station records variations of the vertical component of the electric field coming from a lightning flash. The stations have been equipped with an E-field antenna with a triggering circuit, two-channel data recording device, commercial GPS receiver and a power supply system with a battery backup. The specially constructed data recorders were based on the standard PC/104 built-in computer (AMD LX800 @ 500 MHz) run on Linux operating system. Each recording device has been designed as a stand-alone station working without any operator assistance required during a measurement session. The built-in internal hard drive (~150 GB data buffer) allowed to store the recorded data for 3 days at most, i.e., 72-hour continuous recording in the fast mode with bandwidth up to 100 kHz. The full error analysis of the

best search solution in the case when we had at our disposal six LLDN stations located at different places in the Warsaw region is given by Baranski et al. (2012). This paper also contains a more detailed description of our LLDN recording system performance and its calibration.

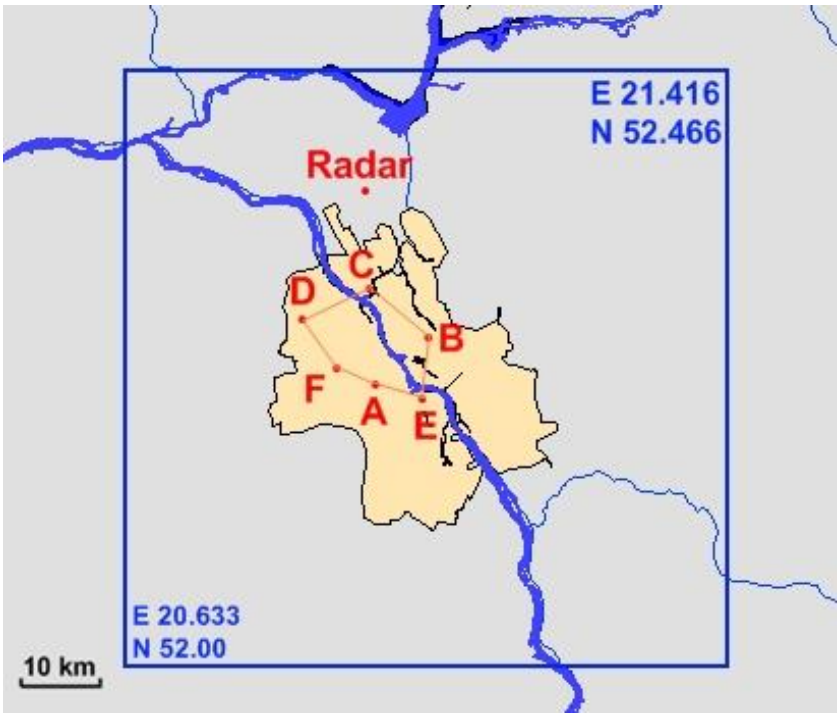

Fig. 1. Location map of six LLDN stations and meteorological radar (METEOR 1500C) set on the background of main rivers around Warsaw together with indication of the area (blue rectangle) covered by additional lightning detections obtained from the PERUN system in Poland.

Fig. 2. The general view of LLDN-F station located at the roof of IG PAS building (20°.939444 E, 52°.245833 N). The GPS/Garmin receiver and E-field antenna sensor mounted on the top of the grey box with the A/D recorder and the power supply buffer inside.

3. SIMULATION SETUP OF THE USED WRF AND WRF_ELEC SCHEME

In this section we present some principal information about the WRF system configuration together with the initial and boundary conditions that are used for the numerical study purpose. The main configuration of the WRF system we used is similar to the one presently applied by Krzyścin et al. (2020) for the comprehensive studies of 24 hr forecast of surface UV radiation in Poland. However, the main difference between these two approaches is connected to the microphysics parameterization. In our study, we used the NSSL microphysics parameterization, which was obligatory for the WRF_ELEC scheme. The NSSL is a 2-moment microphysics scheme, that allows to forecast six different precipitation types (after Mansell et al. 2010 together with Mansell and Ziegler 2013). In the scope of study of the convection weather processes, a graupel and a hail creation is important. Hence, the NSSL for this purpose uses the amount of mass and the number of thundercloud particles. The core of the WRF_ELEC, i.e., the numerical implementation of electric charge separation schemes, is taken from the work of Mansell et al. (2005). Such first implementation into the WRF model was described by Fierro et al. (2013) and included the details of the used basic discharge scheme, i.e., cylindrical discharge regions centered on lightning initiation points.

We implemented the WRF and WRF_ELEC scheme for the purpose of this paper, performing the relevant calculating procedures in three stages listed below.

3.1 The first stage

Here four nesting space domains were used for the WRF simulation. The initial and boundary weather conditions for the first domain (d01) was taken from the NCEP/NCAR Global Reanalysis Products (NCAR 2020). The spatial and temporal resolution for such data was 55×55 km and 1 h, respectively. This domain was implemented for the western and central area of Europe to simulate part of the global atmospheric circulation with a resolution of 12×12 km. The second domain (d02), operated with a resolution of 4×4 km, was dedicated only to the Poland area. The third domain (d03) with an area resolution of 1.333×1.333 km was applied to the Mazovia region and the last (d04), with an area resolution of 0.444×0.444 km, was used for the Warsaw region. For such simulations, the minimal 10-hour spin off was set. For the d01, d02, and d03 domains the 15 minutes temporal resolutions for archiving data was used, but for the d04 domain this time interval was only 1 minute. For all domains, 59 vertical levels were set between 0 and 21 km (a.g.s.l.). Only one nested run of the WRF was used, because farther simulation with the WRF_ELEC with four nested domains connected online between them was not possible. The details of the literature references used for this stage of the conducted evaluations are given in Table 1.

Table 1

The different metrological scheme options used by us for the particular WRF_ELEC procedure calculations with their related literature references

Scheme	
microphysics	NSSL 2-moment (Clark et al. 2012)
longwave radiation	RRTMG (Iacono et al. 2008)
shortwave radiation	Dudhia (Dudhia 1989)
surface layer	Eta similarity (Janjic 1996)
land surface	Pleim-Xu (Pleim and Xu 1995, 2003)
planetary boundary layer	Hong (Hong and Lim 2006)
cumulus	Tiedtke (Tiedtke 1989) only in d01

3.2 The second stage

Here we have used for the WRF_ELEC simulations its model configuration with the scheme details given in Table 2. The choice of such options was strongly imposed by the primary thundercloud electrification solver.

Table 2

The options used by us for the particular WRF_ELEC procedure calculations with their related literature references

Scheme	
nssl_ipelec	non-inductive + inductive charging
nssl_idischarge	discharge turned on
nssl_iscreen	Ziegler et al. (1991)
nssl_lightrad	12000
nssl_disfrac	0.3
nssl_ecrit	120000
nssl_isaund	Brooks et al. (1997)
nssl_ibrkd	Dwyer (2003)

3.3 The third stage

The time intervals used for the numerical calculations for the selected two thunderstorm cases and including the time moment with the occurrence of chosen lightning CG flash are given in Table 3.

Table 3

The indication of time span used in performed relevant simulations together with the time occurrence of two multiple CG flash incidents taken into account

Date of thunderstorm	Start of conducted simulation (UT)	Stop of conducted simulation (UT)	Time of analyzed CG flash incident with limitation to minutes (UT)
25 June 2009	06:00	23:00	16:11
5 July 2009	00:00	23:00	14:41

4. GENERAL CHARACTERISTICS OF MULTIPLE CG FLASHES RETRIEVED FROM LLDN DATABASE AND SELECTED FOR COMPARISON WITH DYNAMIC AND ELECTRIC CHARGE STRUCTURE SIMULATED BY THE WRF AND WRF_ELEC MODELS

Two exemplary cases of multiple CG flashes were selected from the LLDN database obtained in 2009 to be compared with the dynamic and electric charge structure of the particular thundercloud involved in the initiation of the considered CG flash incidents and simulated by the relevant WRF_ELEC modeling. These cases are marked by two blue shaded rows in Table 4.

Table 4

General characteristic parameters of 17 CGs lightning flashes obtained from the LLDN recordings during thunderstorm season in 2009

Flash no. (stroke order/type)	Interstroke intervals [ms]	Δd [km]	Δz [km]	Q_{total} [C]	χ^2 range
#1(1CC,2CC)	22	2.6	0.8	5.02	3÷3.6
#2(1RS,2CC,3CC,4CC)	46.9;59.3;51	12.2	7.5	–15.38	1÷40
#3(1RS,2CC,3CC)	82.7;25	0.5	0.2	–15.35	0.06÷0.3
#4(1RS,2RS,3RS,4RS,5RS,6RS)	23.7;25.8;34.1;11.3;28.9	3.8	5.8	–53.62	0.4÷2
#5(1RS,2RS,3RS)	21.3;10.5	2.7	0.4	–60.77	7÷14
#6(1RS,2RS,3RS)	41.3;28.3	1.0	3.8	–0.53	37.7÷108.9
#7(1RS,2RS,3RS)	57.8;32.9	1.0	1.4	–0.21	92.5÷177.5
#8(1RS,2RS,3RS,4RS,5CC,6RS)	55;36.2;102.7;62.1;148.1	5.7	3.8	–1.21	184.3÷223
#9(1RS,2RS,3RS,4RS)	48.2;30.7;35.1	8.1	5.8	–0.7	38.7÷187.9
#10(1RS,2RS,3RS)	40.8;36.1	0.8	0.5	–0.24	147.8÷187
#11(1RS,2RS)	49.6	4.3	0.2	–0.69	9÷20
#12(1RS,2RS,3RS)	21.2;37.8	2.7	0.1	–1.49	10÷11.6
#13(1RS,2RS,3RS)	52.3;55.9	5	0.9	–1.01	5.5÷9
#14(1RS,2RS,3RS)	70.6;66.3	6.6	0.7	–1.52	3÷6.8
#15(1RS,2RS,3RS)	46.1;66.2	0.4	1.7	–0.42	150.7÷178
#16(1RS,2RS,3RS,4RS)	32.5;64;31,7	6.4	3.4	–0.42	108÷222.8
#17(1RS,2RS)	24.6	1.0	1.7	–0.41	160÷211

Note: RS stands for return stroke, CC for continuing current, Δd for maximum horizontal flash extent, Δz for maximum vertical flash extent, Q total for total charge source of a particular flash.

In turn, the 3D locations together with the amount of electric charge of the particular return stroke sources for flashes #1 and #5 from Table 4 are presented in Figs. 3–4. Such drawings are the result of using the evaluation procedure of space configuration and electric structure of multiple CG flashes described in detail by Baranski et al. (2012).

On the other hand, the relevant WRF simulation of radar reflectivity for the 10 cm radar wavelength and for the thundercloud connected to the case of CG flash #1 is shown in Fig. 5, while in Fig. 6 is presented the related WRF_ELEC simulation of the electric charge density in the considered thundercloud resulting from the used dominant graupel cloud electrification mechanism/scheme and corresponding to the vertical cut along red line given in Fig. 5.

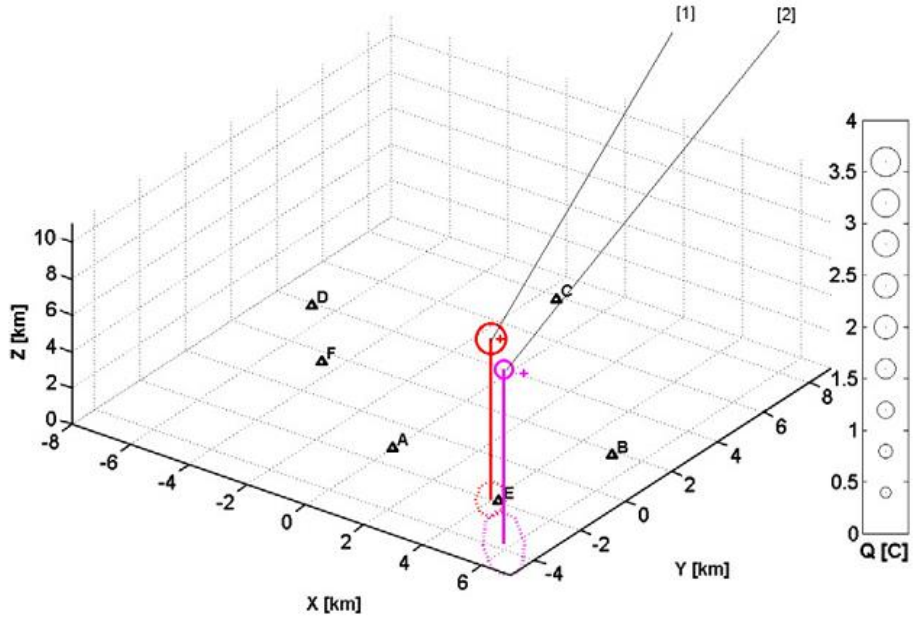

Fig. 3. Example of identification of the electric charge structure of positive multiple CG lightning flash recorded by LLDN in Warsaw during a thunderstorm on 25 June 2009. The first stroke of this flash (in red) was detected at 16:11:57.155491 UTC and the second one (in magenta) at 16:11:57.177478 UTC. Both were recognized as continuing current (CC) stages having charge sources of (3.65±0.59) C and (1.37±0.37) C, at heights, i.e., the z coordinate, (8.8±0.7) km and (9.6±0.6) km, respectively. Capital letters A, B, C, D, E, and F with small triangles indicate locations of the LLDN stations, and the red and magenta ellipses on the XY plane indicate errors of the evaluated x and y coordinates of the charge sources of these CC strokes. The goodness of the (x, y, z, Q) parameter fit was determined by calculating the χ^2 parameter which was equal to 2.5 for the first and 3.6 for the second stroke.

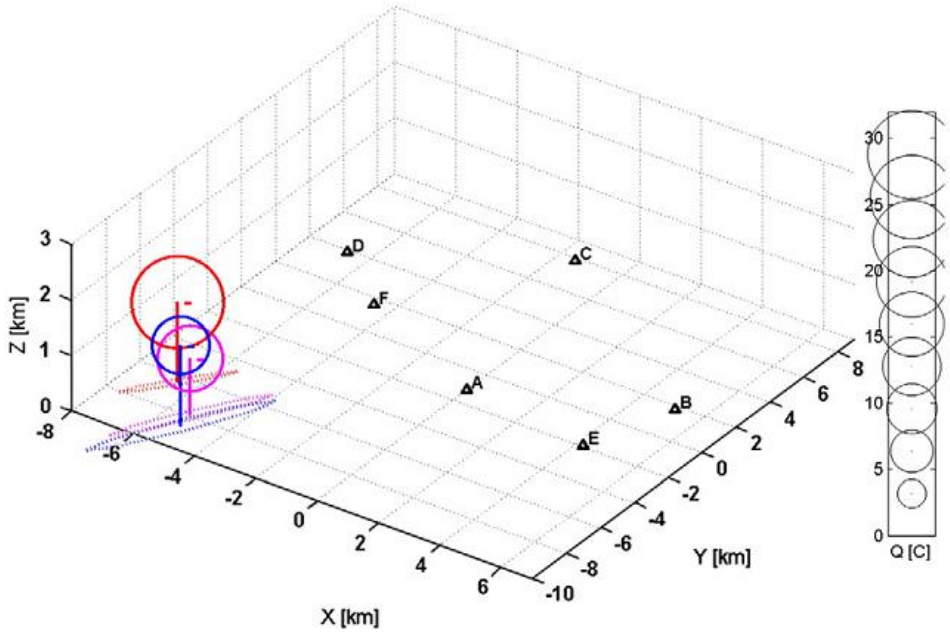

Fig. 4. Multiple negative CG flash consisting of 3 return strokes and distinguished from the LLDN data; denoting key: [red] RS on 5 July 2009, 14:41:14.3479, with x = (−6.6±1.0) km, y = (−6.4±1.7) km, z = (1.4±7.2) km, Q = (−31.75±165.95) C, and χ^2 = 14.0, [magenta] RS on 5 July 2009, 14:41:14.3692, with x = (−5.3±1.2) km, y = (−7.9±2.7) km, z = (1.0±16.4) km, Q = (−16.43±270.21) C, and χ^2 = 7.1, [blue] RS on 5 July 2009, 14:41:14.3797, with x = (−5.2±1.4) km, y = (−8.7±3.2) km, z = (1.4±14.4) km, Q = (−12.59±129.79) C, and χ^2 = 8.3.

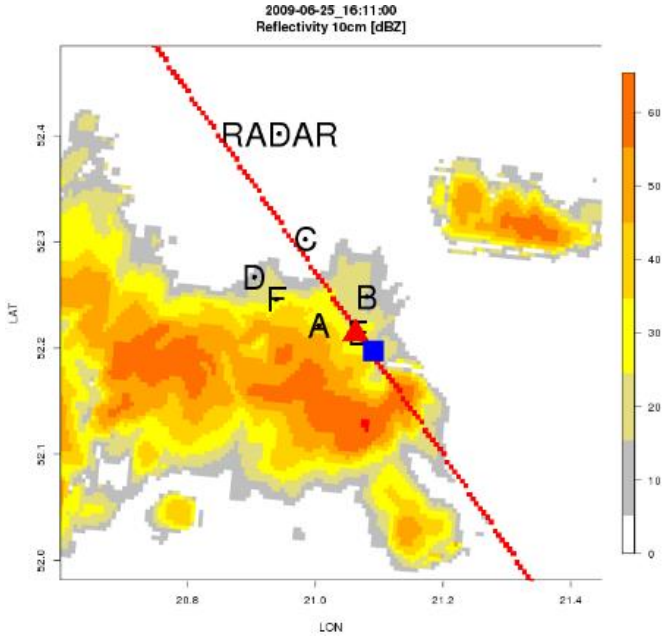

Fig. 5. The WRF simulation of radar reflectivity for the 10 cm radar wavelength and for the thundercloud connected to the case of CG flash #1. The red line is drawn as the best straightforward line fitted to the spread horizontal locations of two positive strokes from this flash and shows the best cross-section line that is used for making the subsequent vertical profile of electric charge density and updraft/downdraft wind pattern in the considered space domain. The first stroke is shown by red triangle and the second by blue square.

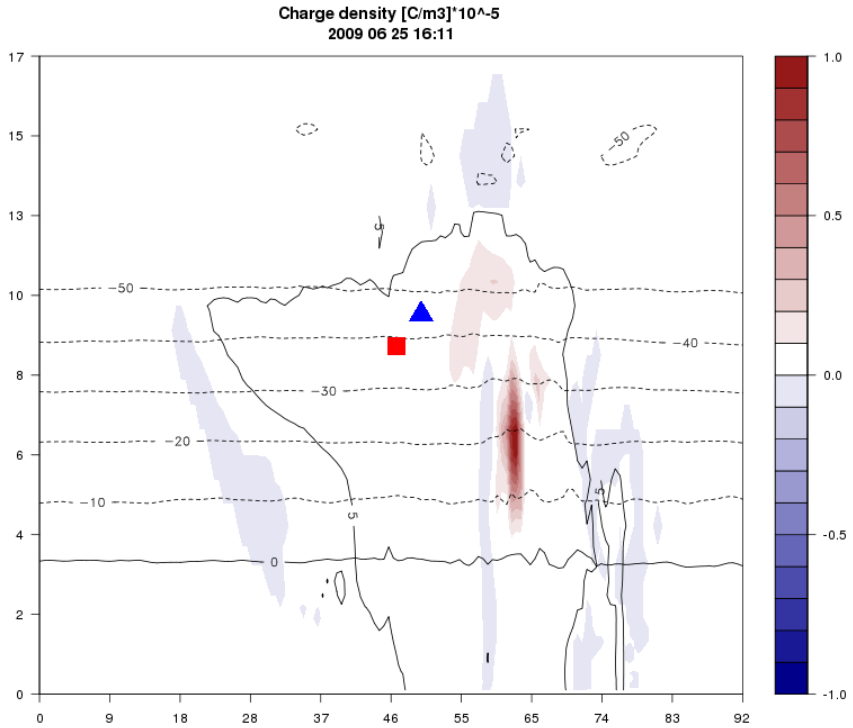

Fig. 6. The WRF_ELEC simulation of the electric charge density in the considered thundercloud resulting from the used dominant graupel cloud electrification mechanism/scheme and corresponding to the vertical cut along the red line shown in Fig. 5 The red triangle and blue square indicates the height of the electric charge source for the first and second stroke of CG flash #1, respectively, and evaluated from the LLDN recordings. The heights of the particular isotherm are given from 0°C by solid black line to –50°C by several black dash lines.

The third kind of performed WRF simulation and referred to the updraft/downdraft wind pattern in the considered thundercloud in the case of CG flash #1, and corresponding to the vertical cut along red line shown in Fig. 5, is depicted in Fig. 7.

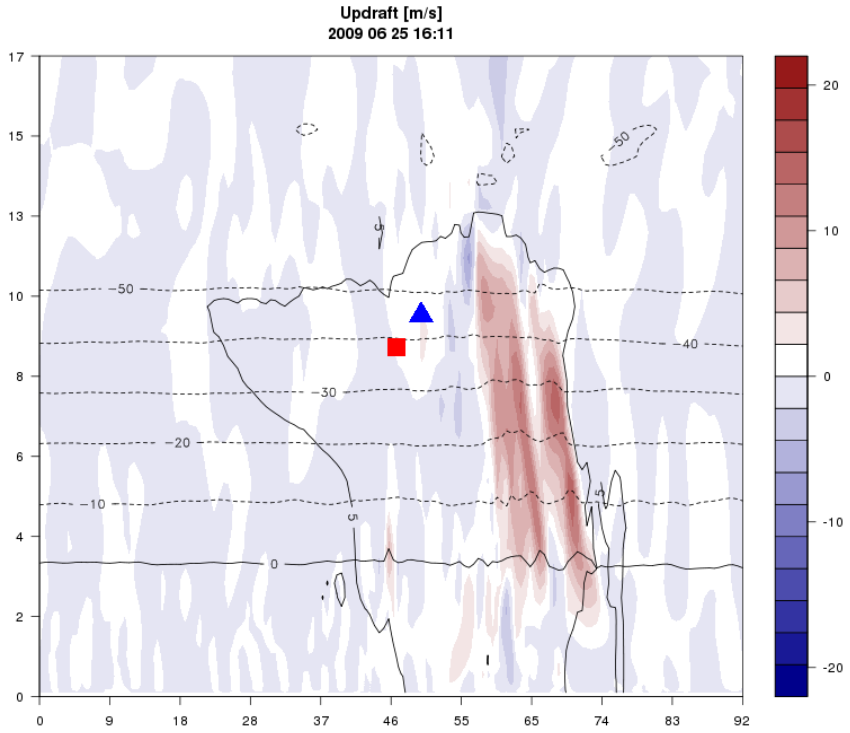

Fig. 7. The WRF simulation of the updraft/downdraft wind pattern in the considered thundercloud and corresponding to the vertical cut along red line shown in Fig. 5. The red triangle and blue square indicates the height of the electric charge source for the first and second stroke of CG flash #1, respectively, and evaluated from the LLDN recordings. The heights of the particular isotherm are given from 0°C by solid black line to –50°C by several black dash lines.

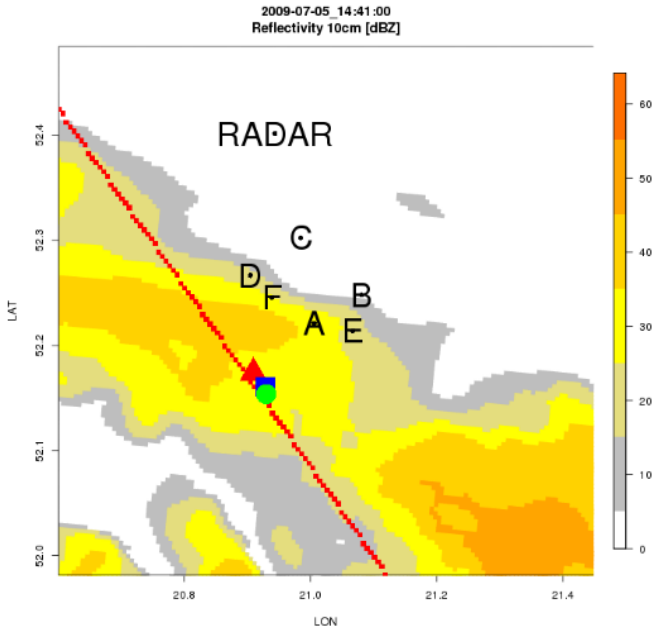

Fig. 8. Same as for Fig. 5, except the case of CG flash #5 with three negative return strokes denoted by red triangle, blue square, and green circle, respectively, and with the new drawn red line shows the best cross-section line belonging to the horizontal locations of these strokes.

The similar set of three following figures, but related to the electric and dynamic conditions of simulated thundercloud and corresponding to the next example of multiple CG flash taken into consideration, i.e., flash #5 from Table 4, is presented in Figs. 8–10.

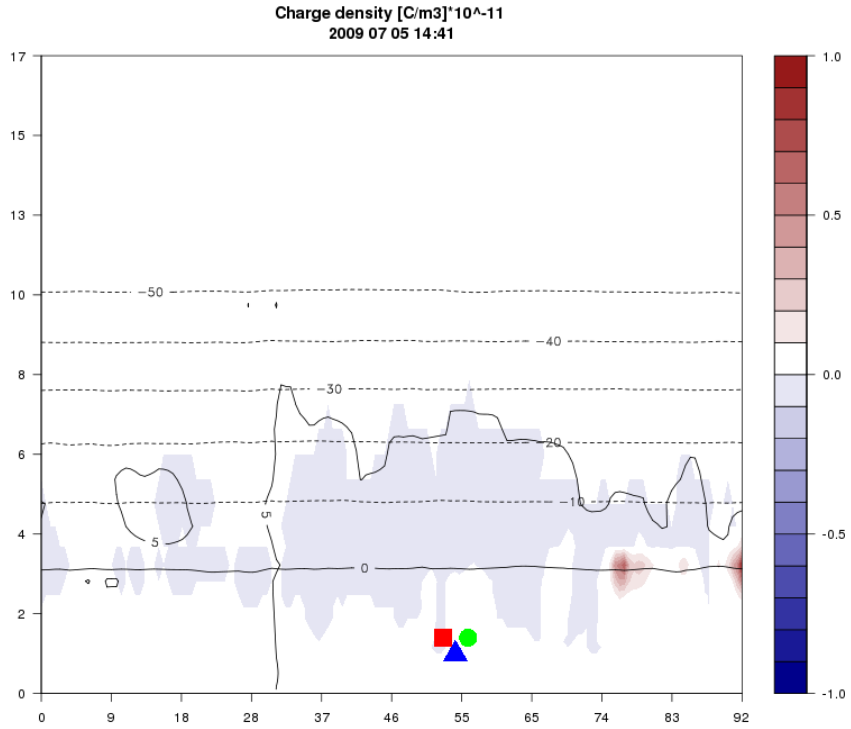

Fig. 9. Same as for Fig. 6, except the newly drawn red line shown in Fig. 8 and the case of CG flash #5 with three negative return strokes denoted by red triangle, blue square, and green circle, respectively, and with their 3D locations evaluated from the LLDN recordings.

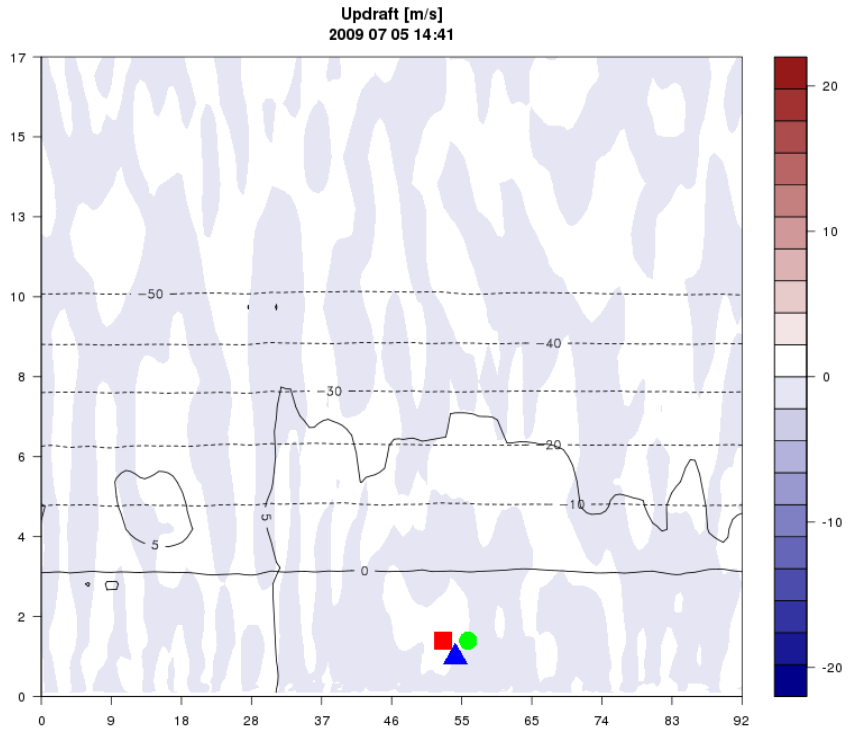

Fig. 10. Same as for Fig. 7, except the case of CG flash #5 with three negative return strokes, but with the new vertical cut along the red line shown in Fig. 8. The red triangle, blue square, and green circle, respectively, and with their 3D locations evaluated from the LLDN recordings.

5. CONCLUSIONS AND FINAL REMARKS

Comparing the 3D locations of the particular stroke from CG flash #1 presented in Fig. 3 and that one shown in Fig. 6 we can notice that these locations evaluated from the LLDN recordings are slightly shifted in relation to the volume of the uppermost positive electric charge near the cloud top and simulated/indicated by the WRF_ELEC model. This shift is less than 9 km. But, if we take into account that these locations evaluated from the LLDN recordings are also having own errors of the order of several kilometers, such a distance difference will be reduced. Moreover, the time simulation given by hours and minutes in Fig. 6 is not the same as this real/exact one with the 0.1 ms accuracy and obtained from the LLDN recordings for the time occurrence of the particular stroke from CG flash #1 (see description of Fig. 3). In that case, the time difference is 57 s. Thus, if we consider the strong updraft with a speed of about 15 m/s and spreading near the cloud top about 1 minute earlier than the exact time of occurrence of the particular stroke from CG flash #1 (see Fig. 6), the considered distance difference will be reduced by about 1 km.

The next comparison concerns the 3D locations of the particular stroke from CG flash #5 presented in Fig. 4 and the one shown in Fig. 9. Here, we have considered the multiple CG flash incident that has occurred below the height of 0°C isotherm and near the cloud base. Both the LLDN recordings and simulations obtained from the used WRF_ELEC model agree/confirm that the initiation of the particular stroke from CG flash #5 is coupled with some negative electric charge volumes appearing near the cloud base and joined to some precipitation shafts (see Fig. 10). For this case, the time difference between the time of the WRF_ELEC simulation and this one for the occurrence of the particular stroke from CG flash #5 (see description of Fig. 4) is only about 14 s. Hence, a possible distance corrections of mutual return stroke locations and displacement of negative electric charge volume evaluated from both methods/ways will be very small, not greater than about 20 m (see Fig. 10 and downdraft speed in the location region of the particular stroke from CG flash #5).

It is worth to note that while the E-field records obtained from the LLDN performance have given us a possibility to evaluate the 3D location and electric charge source of the particular CG stroke according to the one point electrostatic model we used, the conducted WRF_ELEC simulations in the selected vertical cross-section have indicated what kind of electric charge density space distribution/pattern could be involved in such CG flash initiation. These simulations can be carried out with an additional assumption that the inductive or non-inductive processes, or both of them, in the considered thundercloud were responsible for its resultant electrification. On the other hand, the calculated representation/picture of temperature, the updraft/downdraft wind field patterns and the radar reflectivity for 10 cm wavelength delivered by the WRF_ELEC model is supplementary and important information about the microphysical conditions/parameters that may be observed in the surroundings of this electric charge source of the particular lightning stroke detected by the LLDN.

Summarizing, it should be added that both ways of our post-time analysis, i.e., the LLDN recordings of electric field change of return strokes from multiple CG flashes and the results of WRF and WRF_ELEC model simulations, are also allowing to do a supplementary assessment of thundercloud electric charge patterns involved in the initiation of the considered two cases of multiple CG flashes of different polarity, have given coherent final results confirming their suitability and usefulness for future research and location of electric charge sources of ground strokes and dynamic conditions of those thundercloud regions/layers essential for such lightning occurrence. The high time resolution of the WRF and WRF_ELEC simulations of 1 min, i.e., an order of magnitude better than the one routinely available from the IMWM-NRI radar in Legionowo, is also important and valuable improvement in such examinations.

Acknowledgments. This work was partially supported within statutory activities No. 3841/E-41/S/2020 of Poland's Ministry of Education and Science.

References

Baranski, P., M. Loboda, J. Wiszniowski, and M. Morawski (2012), Evaluation of multiple ground flash charge structure from electric field measurements using the local lightning detection network in the region of Warsaw, *Atmos. Res*. **117**, 99–110, DOI: 10.1016/j.atmosres.2011.10.011.

Brooks, I.M., C.P.R. Saunders, R.P. Mitzeva, and S.L. Peck (1997), The effect on thunderstorm charging of the rate of rime accretion by graupel, *Atmos. Res*. **43**, 3, 277–295, DOI: 10.1016/S0169-8095(96)00043-9.

Clark, A.J., S.J. Weiss, J.S. Kain, I.L. Jirak, M. Coniglio, Ch.J. Melick, Ch. Siewert, R.A. Sobash, P.T. Marsh, A.R. Dean, M. Xue, F. Kong, K.W. Thomas, Y. Wang, K. Brewster, J. Gao, X. Wang, J. Du, D.R. Novak, F.E. Barthold, M.J. Bodner, J.J. Levit, C.B. Entwistle, T.L. Jensen, and J. Correia Jr. (2012), An overview of the 2010 hazardous weather testbed experimental forecast program spring experiment, *Bull. Am. Meteorol. Soc*. **93**, 1, 55–74, DOI: 10.1175/BAMS-D-11-00040.1.

Dudhia, J. (1989), Numerical study of convection observed during the winter monsoon experiment using a mesoscale two-dimensional model, *J. Atmos. Sci*. **46**, 20, 3077–3107, DOI: 10.1175/1520-0469(1989)046<3077:NSOCOD>2.0.CO;2.

Dwyer, J.R. (2003), A fundamental limit on electric fields in air, *Geophys. Res. Lett*. **30**, 20, 2055, DOI: 10.1029/2003GL017781.

Fierro, A.O., E.R. Mansell, D.R. MacGorman, and C.L. Ziegler (2013), The implementation of an explicit charging and discharge lightning scheme within the WRF-ARW model: Benchmark simulations of a continental squall line, a tropical cyclone, and a winter storm, *Mon. Weather Rev*. **141**, 7, 2390–2415, DOI: 10.1175/MWR-D-12-00278.1.

Hong, S.Y., and J.O.J. Lim (2006), The WRF single-moment 6-class microphysics scheme (WSM6), *J. Korean Meteor. Soc*. **42**, 2, 129–151.

Iacono, M.J., J.S. Delamere, E.J. Mlawer, M.W. Shephard, S.A. Clough, and W.D. Collins (2008), Radiative forcing by long-lived greenhouse gases: Calculations with the AER radiative transfer models, *J. Geophys. Res.: Atmos*. **113**, D13, D13103, DOI: 10.1029/2008JD009944.

Janjic, Z.I. (1996), The surface layer in the NCEP Eta Model. **In:** *11th Conference on Numerical Weather Prediction, August 19–23, Norfolk, VA*, American Meteorological Society, Boston, 354–355.

Krzyścin, J.W., J. Guzikowski, A. Pietruczuk, and P.S. Sobolewski (2020), Improvement of the 24 hr forecast of surface UV radiation using an ensemble approach, *Meteorol. Appl*. **27**, 1, 1350–4827, DOI: 10.1002/met.1865.

Mansell, E.R., and C.L. Ziegler (2013), Aerosol effects on simulated storm electrification and precipitation in a two-moment bulk microphysics model, *J. Atmos. Sci*. **70**, 7, 2032–2050, DOI: 10.1175/JAS-D-12-0264.1.

Mansell, E.R., D.R. MacGorman, C.L. Ziegler, and J.M. Straka (2005), Charge structure and lightning sensitivity in a simulated multicell thunderstorm, *J. Geophys. Res.: Atmos*. **110**, D12, D12101, DOI: 10.1029/2004JD005287.

Mansell, E.R., C.L. Ziegler, and E.C. Bruning (2010), Simulated electrification of a small thunderstorm with two-moment bulk microphysics, *J. Atmos. Sci*. **67**, 1, 171–194, DOI: 10.1175/2009JAS2965.1.

NCAR (2020), National Centers for Environmental Prediction/National Weather Service/NOAA/U.S. Department of Commerce: NCEP/NCAR Global Reanalysis Products, 1948-continuing, Re-

search Data Archive at the National Center for Atmospheric Research, Computational and Information Systems Laboratory, available from: https://rda.ucar.edu/datasets/ds090.0/ (accessed: 30 September 2020).

Pleim, J.E., and A. Xiu (1995), Development and testing of a surface flux and planetary boundary layer model for application in mesoscale models, *J. Appl. Meteorol*. **34**, 1, 16-32.

Pleim J.E., and A. Xiu (2003), Development of a land surface model. Part II: Data assimilation, *J. Appl. Meteorol. Climatol*. **42**, 12, 1811–1822, DOI: 10.1175/1520-0450(2003)042<1811:DOALSM>2.0.CO;2.

Tiedtke, M. (1989), A comprehensive mass flux scheme for cumulus parameterization in large-scale models, *Mon. Weather Rev*. **117**, 8, 1779–1800, DOI: 10.1175/1520-0493(1989)117<1779:ACMFSF>2.0.CO;2.

Ziegler, C.L., D.R. MacGorman, J.E. Dye, and P.S. Ray (1991), A model evaluation of noninductive graupel-ice charging in the early electrification of a mountain thunderstorm, *J. Geophys. Res.: Atmos*. **96**, D7, 12833–12855, DOI: 10.1029/91JD01246.

Received 16 September 2022
Received in revised form 28 December 2022
Accepted 31 December 2022